TRENDS IN SCIENCES 2026; 23(6): 12794
https://doi.org/10.48048/tis.2026.12794 RESEARCH ARTICLE

Structural-Functional Analysis and Response Surface Methodology (RSM) Modelling of Chitosan-Botanical Extract Edible Coatings and Films

Edo Saputra[1,4,*], Rokhani Hasbullah[2], Emmy Darmawati[2] and Mala Nurilmala[3]

[1]*Agricultural Engineering Study Program, Faculty of Agricultural Engineering and Technology, IPB University, Bogor 16680, Indonesia*
[2]*Department of Mechanical and Biosystem Engineering, Faculty of Agricultural Engineering and Technology, IPB University, Bogor 16680, Indonesia*
[3]*Department of Aquatic Product Technology, Faculty of Fisheries and Marine Science, IPB University, Bogor 16680, Indonesia*
[4]*Department of Agricultural Technology, Faculty of Agriculture, Universitas Riau, Pekanbaru 28293, Indonesia*

([*]Corresponding author's e-mail: edosaputrasaputra@apps.ipb.ac.id)

Received: 25 November 2025, Revised: 13 December 2025, Accepted: 23 December 2025, Published: 15 February 2026

Abstract

Demand for bioactive edible coatings and films from renewable biopolymers is increasing due to the need for sustainable alternatives to synthetic plastics. However, achieving formulations that simultaneously optimize mechanical strength, flexibility, and stability of bioactive compounds remains a challenge. This study introduces a novel approach by integrating 3 spice extracts-garlic, red ginger, and red galangal as synergistic reinforcers within a chitosan matrix for edible coating and film systems, modelled through a custom Response Surface Methodology (RSM) design. This study aims to investigate interactive effects between chitosan concentration, extract proportion, and glycerol plasticization on structural performance and bioactive functionality. Fresh extracts of garlic, red ginger, and red galangal were prepared without solvents and combined with chitosan solutions at varying concentrations. Formulations for films included glycerol as a plasticizer, whereas coating formulations excluded glycerol. Results demonstrated that variations in chitosan and extract concentrations significantly influenced pH, antimicrobial activity, tensile strength, and elongation. FTIR analysis confirmed enhanced hydrogen bonding and matrix reinforcement through phenolic-based interactions, explaining improved flexibility and mechanical stability. Conversely, antioxidant activity and inhibition against *S. aureus* showed non-significant differences across formulations, indicating different sensitivity mechanisms. The RSM model produced highly valid predictive equations for linear, quadratic, and 2FI interaction responses, with strong goodness of fit parameters. The optimal formulation, consisting of 1.33% chitosan and 33.3% extract, generated a balanced performance indicated by pH 4.31, IC_{50} 4.43 ppm, inhibition zones against *E. coli* 2.32 mm, *S. aureus* 4.70 mm, *Salmonella* 5.23 mm, thickness 0.18 mm, tensile strength 5.01 MPa, elongation 6.00%, and WVTR 252.74 $g \cdot day^{-1} \cdot m^{-2}$. These findings provide strong evidence that combining multiple spice extracts within a chitosan matrix improves antimicrobial strength and mechanical flexibility without compromising stability. This study establishes an innovative formulation strategy with significant potential for scalable production of sustainable edible coatings and films as eco-friendly packaging materials.

Keywords: Custom design, Chitosan extract, Edible coating, Edible film, FTIR, RSM

Introduction

Interest in the use of edible coatings and films based on biopolymers is increasing, aligning with global demands to reduce the use of synthetic plastics and provide packaging materials that are safe, natural, environmentally friendly, and sustainable. Biopolymer-based coatings from renewable sources offer more substantial environmental benefits than synthetic

polymers because they degrade naturally and effectively reduce pollution [1]. In addition, edible coatings are capable of forming a solid matrix based on biopolymers and adaptogens that function as carriers of bioactive compounds and provide antimicrobial and biodegradable properties. Developments in edible coating technology show a shift from the use of synthetic materials to a safer biological approach, with a focus on improving physical, mechanical, and water vapor barrier properties [2]. However, developing an optimal formulation remains a challenge because it requires a balance between strength, flexibility, and surface stability, thus requiring edible coating characteristics that demand the selection of biopolymers with superior structural functions, abundant raw materials, and easy availability [3].

Among the various biopolymers studied, chitosan is a prominent candidate due to its antimicrobial activity, film-forming ability, non-toxicity, easily modifiable chemical structure, and biodegradability [4-6]. These characteristics enable chitosan to function effectively as a carrier matrix for active compounds, such as antimicrobial and antioxidant properties [7], while also providing environmentally friendly properties [8], an effective barrier against O_2 and CO_2 [9], and contributing to hydrophobic properties [10]. However, the limitations of chitosan, namely its low flexibility and limited moisture barrier properties [11], remain a significant obstacle, requiring formulation modification strategies. Bioactive compounds rich in phenolics and flavonoids strengthen the matrix structure and increase the functional performance of polymer film coatings. Extracts of garlic (*Allium sativum*), red ginger (*Zingiber officinale* var. *rubrum*), and red galangal (*Alpinia purpurata*) are potential candidates for improving the physical properties and stability of chitosan-based coatings.

Based on their mechanism of action, the positively charged amine groups in chitosan can bind to the negatively charged phenolic and flavonoid compounds in plant extracts, thereby forming a denser matrix network. This interaction contributes to increased mechanical strength, reduced water vapour and oxygen permeability, and slowed oxidative degradation. A combination of chitosan's ability to damage microbial cell membranes and the inhibition of microbial respiration enzymes by bioactive compounds in plant extracts generates vigorous synergistic antimicrobial activity. Various studies have shown that essential oils and extracts of garlic, red ginger, and red galangal can improve the functional properties, antimicrobial activity, antioxidant activity, and physical, mechanical, and permeability properties of edible films [12-22]. However, most studies only evaluate physicochemical and bioactive properties linearly, without examining structure-function mechanisms or modelling interactions between formulation variables that can produce non-linear responses. Furthermore, no published work simultaneously optimizes the combination of these 3 extracts as chitosan matrix reinforcers in edible coating and edible film systems. This gap highlights the need for a statistical modelling approach that can comprehensively evaluate linear, interaction, and quadratic effects to predict coating characteristics and determine optimal conditions accurately.

This study applies the Response Surface Methodology (RSM) with a custom design to model the responses of edible coating and edible film treatments based on chitosan-spice extract. This approach was chosen because previous studies were still descriptive and assessed the effects of the formulation linearly, without evaluating the structure-function mechanism and without modeling variable interactions that could produce linear responses. This gap requires a statistical modeling approach that can comprehensively evaluate linear, interaction, and quadratic effects to predict the characteristics of edible coatings and films accurately. RSM is an experimental design approach based on statistical-mathematical modelling used to describe the measurable relationship between parameters and responses [13]. The empirical approach based on polynomial regression is capable of evaluating linear, interaction, and quadratic effects simultaneously, enabling rapid, efficient, and economical modelling and optimization when the underlying mechanism model is not available [23]. In the context of this study, predictive equations serve not only as prediction tools but also as quantitative frameworks for elucidating the mechanisms of improvement in physical, chemical, and bioactive properties resulting from the combination of chitosan and extracts. This directly highlights the main scientific contribution of the study, namely the integration of empirical data with validated predictive models. The

custom design approach was chosen because the experimental conditions involving edible coatings and edible films based on chitosan-spice extracts did not fully comply with the classical RSM design, thus requiring a more flexible design to produce a valid and relevant predictive model. Unlike previous studies that focused on essential oils, this study adopted a natural extract-based approach, which resulted in a more complex composition of active compounds and had the potential to provide stronger structural interactions with the chitosan matrix. The selection of extracts was based on their simpler and more practical processing, as well as their ability to form synergistic interactions with the amino groups of chitosan, thereby improving the stability of the matrix and the functional characteristics of the coating. To our knowledge, this approach has not been reported previously, thus providing a new contribution to the development of biopolymer-based active coating systems, particularly through the use of a combination of 3 phenolic-rich extracts as chitosan matrix reinforcers. This study aims to examine the physical, chemical, and bioactive characteristics of edible coatings and edible films based on chitosan-spice extracts, and to model them through the application of RSM with a custom design to explain the interaction between formulation variables and predict coating characteristics more accurately, while providing practical recommendations for the development of sustainable food packaging. The main findings of the study are not merely descriptive, but are reflected in the coefficients and constants of the predictive equation developed. The equation provides a quantitative framework for the mechanism of improving the properties of coatings and edible films, while strengthening the connection between empirical data and verified models. Thus, the results of this study confirm a systematic transition from experimental observation to a reliable predictive approach.

Materials and methods

Materials

This study used chitosan sourced from vanamei shrimp shells (*Litopenaeus vannamei*). Fresh garlic (*Allium sativum* L.), red ginger (*Zingiber officinale* var. *rubrum*), and red galangal (*Alpinia purpurata* K. Schum.) came from local markets in Pekanbaru, Indonesia. The preparation process applied glacial acetic acid as the chitosan solvent, glycerol as the plasticizer, and distilled water as the base solvent. Additional chemicals included DPPH reagent (2,2-diphenyl-1-picrylhydrazyl, 95% purity), 96% ethanol, and sodium chloride, while microbiological media included Mueller-Hinton Agar and Plate Count Agar. All materials met pro-analytical grade quality standards (E-Merck, Darmstadt, Germany). The antimicrobial testing used isolates of *E. coli* (Gram-negative), *S. aureus* (Gram-positive), and *Salmonella* (Gram-negative from the culture collection of the Agricultural Microbiology Laboratory, Andalas University, Padang, Indonesia, through the disc diffusion method.

Preparation of garlic, red ginger, and red galangal extracts

The extraction process used fresh materials without solvents through the juicing method, following Akullo *et al.* [24] with modifications. The procedure filtered the pure extract and stored it in a sealed container in a dark room. The formulation applied a composition ratio of 25% garlic, 50% red ginger, and 25% red galangal, selected based on physical stability and bioactive activity results that delivered the most consistent and effective performance in the system.

Formulation and preparation of chitosan-based edible coatings and edible films with combined extracts

The formulation used chitosan solutions at concentrations of 2.00% - 4.00% (w/v combined with extracts at concentrations of 0% - 33.3% [25,26] to produce edible coatings and edible films. The coating system applied 6 chitosan concentration levels and 3 extract concentrations. The film used the same formulation combination and incorporated 30% glycerol by weight of chitosan as a plasticizer [27]. The process homogenized all solutions until thoroughly mixed, then applied them as surface coatings or poured them into molds to form films. The material dried at room temperature until it formed a smooth layer without air bubbles. The final product remained in sealed containers prior to analysis.

Experimental design

This study employed a Completely Randomized Design (CRD) factorial to evaluate the effect of

variations in chitosan-based formulations on the characteristics of edible coatings and films. The first factor is the chitosan concentration, with 6 levels: 2.00%, 1.60%, 1.33%, 4.00%, 3.20%, and 2.67% (w/v). The second factor is the extract concentration, with 3 levels: 0%, 20%, and 33.3% (v/v). For edible film, a third factor was added, namely glycerol as a plasticizer at 2 levels: Without glycerol and with 30% glycerol of the chitosan weight. The combination of these factors resulted in 6 treatments for edible coating and twelve treatments for edible film, each repeated 3 times to obtain valid quantitative data for statistical analysis.

Response surface methodology design (RSM)

The study modelled all treatments using RSM with a custom design approach, enabling flexible evaluation of linear, quadratic, and 2-factor interaction (2FI) effects. The modelling process used Design Expert 13 software (Stat-Ease Inc., USA) to obtain the most accurate mathematical representation for predicting the primary response. The evaluation compared several model forms (linear, 2FI, and quadratic) and progressively removed insignificant variables to enhance model suitability for the data. The analysis assessed modelling quality through *lack of fit* testing, the *coefficient of determination* (R^2), *adjusted* R^2, *prediction* R^2, and *adequate precision* to ensure accurate and consistent prediction performance. Response surface plots illustrated the interactions among factors, with other factors fixed at optimum conditions or relevant reference levels. The final model selection relied entirely on the statistical recommendations generated from the software according to parameter fit and significance, and the custom design applied the quadratic model described in Eq. (1).

$$Y = \beta_0 + \sum_{i=1}^{k} \beta_i X_i + \sum_{i=1}^{k} \beta_{ii} X_i^2 + \sum_{i=1}^{k-1} \sum_{j=1+1}^{k} \beta_{ij} X_i X_j + \varepsilon \quad (1)$$

where Y represents the predicted response, β_0 is the intercept (constant coefficient), β_i is the linear coefficient, X_i is the i-th factor, β_{ii} is the quadratic coefficient, β_{ij} is the interaction coefficient, X_iX_j is the combination of independent variables, k is the number of factors, and ε is the random error arising from the experimental data.

Acidity level (pH)

The pH of the edible coating solution was measured using a calibrated pH meter, following the method described in Pažarauskaitė *et al*. [28] with modifications. Each treatment was measured in triplicate to ensure consistency of results.

Antioxidant activity (IC_{50})

The analysis measured the antioxidant activity of the edible coating using the DPPH method based on Pažarauskaitė *et al*. [28] with modifications. The procedure extracted the samples in ethanol and reacted them with the DPPH solution, then incubated the mixture in dark conditions at room temperature. The spectrophotometer recorded absorbance at 517 nm, and the measurements used 3 replicates to ensure accuracy. A DPPH solution without samples functioned as the control. The calculation expressed antioxidant activity as the percentage of free radical scavenging activity using Eq. (2).

$$\text{DPPH scavenging activity (\%)} = \frac{A_{control} - A_{sample}}{A_{control}} \quad (2)$$

where $A_{control}$ is the absorbance of the control (ethanol + DPPH), and A_{sampel} is the absorbance of the sample after incubation.

Antimicrobial activity

The analysis evaluated the antimicrobial activity of the edible coating against *E. coli* (Gram-negative), *S. aureus* (Gram-positive), and *Salmonella* (Gram-negative), which represent major foodborne pathogens as reported by Dysjaland *et al*. [29]. The procedure used the disk diffusion method on Mueller-Hinton Agar, with discs soaked in the edible coating solution. After incubation at 37 °C for 24 h, the observation focused on inhibition zones around the discs as indicators of antibacterial activity. The procedure measured the diameter of each inhibition zone and recorded the results as the mean ± standard deviation from 3 replicates. Larger inhibition zones signified stronger antibacterial efficacy of the edible coating formulations.

Fourier transform infrared spectroscopy (FTIR)

The analysis characterized the edible coating using FTIR to identify functional groups and evaluate physicochemical properties according to the method described in [30]. The procedure applied the Attenuated Total Reflectance (ATR) technique in the infrared range of 400 - 4,000 cm^{-1} with a resolution of 4 cm^{-1} through 32 scans. The instrument collected the spectral data and interpreted the results using the standard built-in software.

Thickness

The film thickness was measured using a screw micrometer with a precision of 0.01 mm [31,32]. The procedure measures thickness at 3 different points and then computes the average value using Eq. (3).

$$\text{Thickness (mm)} = \frac{a + b + c}{3} \quad (3)$$

where a and b are the thicknesses at the ends, and c is the thickness at the midpoint.

Tensile strength and elongation

Tensile strength and elongation tests follow the ASTM D882 method using a standard testing machine [32,33]. The tensile strength derives from the maximum force the film withstands before breaking, while the elongation comes from the change in film length after breaking relative to its initial length. The calculation of these 2 parameters refers to Eqs. (4) and (5).

$$KT = \frac{F}{A} \quad (4)$$

$$E = \frac{L_1 - L_0}{L_0} \quad (5)$$

where KT is tensile strength (MPa), F is tensile force (N), A is film surface area (m^2), E is elongation (%), is initial film length (mm), and L_1 is film length after breaking (mm).

Water vapor transmission rate (WVTR)

Water vapor transmission rate measurements were performed gravimetrically based on the ASTM E96-05 method with modifications [34]. The film covers a dish filled with silica gel, and the dish sits inside a desiccator containing a NaCl solution that creates a controlled vapor pressure gradient between the inside and outside of the dish. Periodic mass measurements of the dish provide the data needed to determine the WVTR value using Eq. (6).

$$\text{WVTR (g day}^{-1}\text{m}^{-2}) = \frac{\Delta n}{t \times A} \quad (6)$$

where Δn is the change in weight of porcelain dish (g), t is the time interval (hours), and A is the surface area of the film (m^2)

Statistical analysis

Statistical analysis uses SPSS software version 25 (IBM, Chicago, IL, USA) to process the data. Data were analysed using 2-way analysis of variance (ANOVA) to evaluate the effects of primary factors and interactions between factors on the characteristics of edible coatings and edible films. The Tukey test was used as a post hoc test when significant differences were found, with a significance level set at $p < 0.05$. A custom RSM design models the main responses to evaluate the linear, quadratic, and interaction effects of the formulation factors. Model performance relies on *lack of fit* analysis, R^2, *adjusted* R^2, *predicted* R^2, and *adequate precision* values to determine overall quality.

Results and discussion

Table 1 presents the pH, antioxidant activity, and antimicrobial activity of the edible coating formulations evaluated in this study. The pH value reflects the stability of the colloidal system and the potential for chemical interaction between chitosan and active compounds. At the same time, antioxidant activity indicates the coating's ability to suppress oxidative damage to the product. The assessment of antimicrobial activity involves measuring the inhibition-zone diameter against *E. coli*, *S. aureus*, and *Salmonella*, which indicates how effectively each coating formulation suppresses the growth of these microorganisms. **Figure 1** shows 3-dimensional (3D) response surface plots that illustrate the effect of chitosan and extract concentrations on pH, antioxidant activity, and antimicrobial activity. This visualization confirms the interaction between formulation variables

that affect system stability, the coating's ability to suppress oxidation, and the effectiveness of microorganism inhibition. **Figure 2** shows the visualization of the inhibition zone of each treatment, which provides visual evidence of the antimicrobial effectiveness of the chitosan-natural extract-based edible coating. These 3 parameters (pH, antioxidant activity, and antimicrobial activity) synergistically determine the stability and functional effectiveness of the developed coating. **Table 2** presents the ANOVA and regression results of the RSM model, which can accurately predict pH, antioxidant activity, and antimicrobial activity, while also identifying the interactive effects of chitosan and extract concentrations on the functional characteristics of the edible coating.

Table 1 pH, antioxidant activity, antimicrobial activity (*E. coli*, *S. aureus*, *Salmonella*) of edible coating.

Treatment		Parameter				
Chitosan concentration (% w/v)	**Extract (% v/v)**	**pH**	**Antioxidant activity (ppm)**	***E. coli* (mm)**	***S. aureus* (mm)**	***Salmonella* (mm)**
2	0	3.75 ± 0.06^{a}	11.54 ± 5.09	2.35 ± 0.72^{ab}	2.60 ± 0.69	1.67 ± 1.07^{a}
1.6	20	4.08 ± 0.05^{b}	6.31 ± 3.60	1.30 ± 0.80^{a}	4.00 ± 0.68	6.90 ± 0.00^{d}
1.33	33.3	4.31 ± 0.01^{cd}	4.43 ± 2.69	2.32 ± 0.36^{ab}	4.70 ± 1.73	5.23 ± 0.39^{cd}
4	0	4.20 ± 0.05^{bc}	9.15 ± 2.69	2.17 ± 0.26^{ab}	2.67 ± 0.83	2.10 ± 0.91^{ab}
3.2	20	4.36 ± 0.04^{d}	5.12 ± 0.33	2.17 ± 0.23^{ab}	2.13 ± 1.27	2.98 ± 1.19^{ab}
2.67	33.3	4.56 ± 0.03^{e}	5.77 ± 2.75	3.58 ± 0.92^{b}	2.65 ± 0.61	3.90 ± 0.00^{bc}

The data present values as mean ± SD (n = 3), and different lowercase letters in each column indicate significant differences ($p < 0.05$) according to Tukey's post-hoc test.

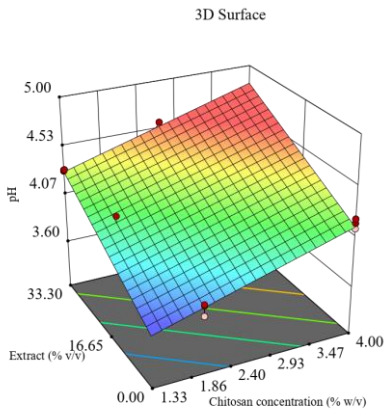

(A)

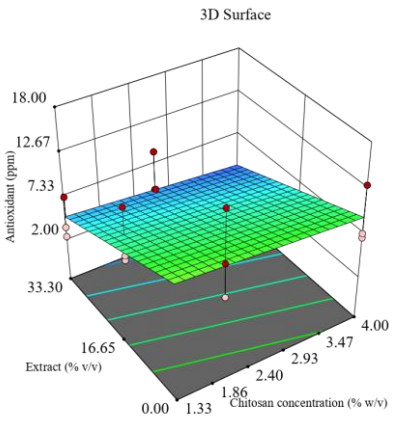

(B)

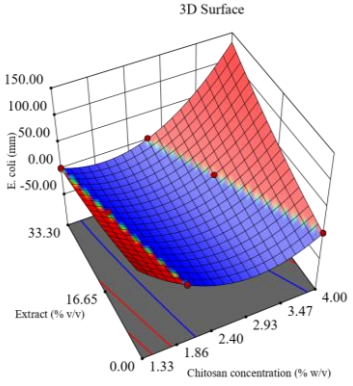

(C)

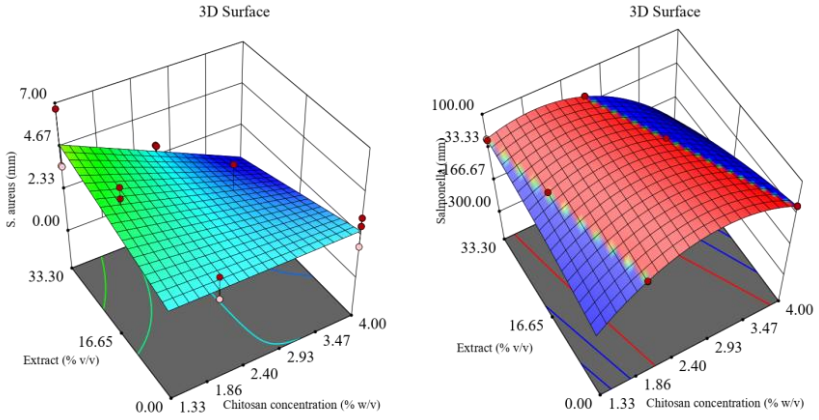

(E) **(F)**

Figure 1 Surface response plot of the effect of chitosan and extract concentration on: (A) pH, (B) antioxidant activity, (C) *E. coli*, (D) *S. aureus*, and (E) *Salmonella*.

pH

The concentration of chitosan and the extract ratio significantly affected the pH value of the edible coating ($p < 0.05$), as shown in **Table 1**. An increase in the concentration of natural extracts in the coating system consistently led to an increase in pH, with a significant difference between formulations without extracts and those with high extract concentrations. The fundamental nature of the extract explains this mechanism, as the extract lowers the protonation level of chitosan's amine groups and consequently reduces the acidity of the solution. This change in pH has a direct implication on the stability of the coating structure and the intensity of ionic interactions in the chitosan-extract matrix. This trend confirms that the composition of the formulation, particularly the proportion of chitosan and extract, plays a role in determining the acid-base characteristics of the coating. The amino groups of chitosan interact with the carboxyl groups and phenolic compounds of bioactive compounds, thereby contributing to the ionic stability of the solution and increasing the pH measurably. Formulations with a higher extract ratio produced a higher pH in the chitosan matrix, presumably due to ionic interactions and increased electron density from phenolic compounds. The increase in pH in the chitosan-extract formulation directly reduces the number of positively charged $-NH_3^+$ groups. This change explains the measurable increase in pH in the system while reflecting its ionic nature [35]. The addition of bioactive extracts to the edible coating matrix affects pH changes through phenolic-amine interactions with chitosan, which can either inhibit or reduce the increase in pH [36].

ANOVA analysis (**Table 2**) shows that the linear model significantly explains the effect of chitosan and extract concentrations on the pH of the coating solution ($p < 0.0001$). Both factors make a significant contribution and alter the pH response. The lack of fit value of 0.4609 ($p > 0.05$) confirms that the model does not experience systematic deviation and can represent data variation well. The coefficient of determination (R^2 = 0.9729), *adjusted* R^2 (0.9693), and *predicted* R^2 (0.9600) indicate the stability and high accuracy of the model, reinforced by an *adequate precision* value (42.2982) that indicates excellent predictive consistency. The 3D plot (**Figure 1(A)**) shows that an increase in chitosan concentration raises the pH, while the extract lowers it within a specific range. The interaction between the 2 affects the acidity of the solution, with blue-red color degradation reflecting an increase in pH due to the fundamental nature of chitosan and the presence of phenolic compounds and organic acids from the extract. This pattern indicates a synergistic effect between the 2 factors on the acidity characteristics of the system. Eq. (7) presents the regression equation used to predict the pH of the edible coating.

$$pH = 3.3337 + 0.2005A + 0.0199B \quad (7)$$

Table 2 ANOVA results and RSM model regression for pH, antioxidant activity, and antimicrobial activity prediction.

Response	pH	Antioxidant activity	*E. coli*	*S. aureus*	*Salmonella*
Model (Reduction/Transformation)	Linear	Linear	Quadratic	2FI	Quadratic
Model (*p*-value)	< 0.0001	0.0253	0.0114	0.0142	0.0012
Chitosan concentration (A)	< 0.0001	0.5217	0.3160	0.0112	0.2925
Extract (B)	< 0.0001	0.0091	0.3137	0.9751	0.3226
AB	na	na	0.3257	0.0280	0.3066
A^2	na	na	0.3324	na	0.3129
B^2	na	na	0.2657	na	0.2580
Lack of fit (*p*-value)	0.4609	0.6981	0.9031	0.7878	0.0239
R^2	0.9729	0.3876	0.6706	0.5193	0.7807
Adjusted R^2	0.9693	0.3059	0.5334	0.4163	0.6893
Predicted R^2	0.9600	0.0650	0.3152	0.1700	0.5350
Adequate precision	42.2982	5.0001	7.4209	5.8147	6.7020

na = not applicable, R^2 = coefficient of determination

Antioxidant activity

The DPPH free radical scavenging assay measures antioxidant activity, using IC_{50} as the primary indicator. The IC_{50} value reflects the concentration of the sample required to neutralise 50% of free radicals, so a lower IC_{50} value indicates higher antioxidant capacity. The IC_{50} value of the edible coating showed variations depending on the concentration of chitosan and extract used. Antioxidant activity showed a decreasing trend as the ratio of natural extract in the edible coating formulation increased. However, higher chitosan concentrations were able to maintain some of their antioxidant capacity (**Table 1**). Statistically, there were no significant differences between treatments ($p > 0.05$), so variations in chitosan and extract did not significantly affect antioxidant activity. However, the downward trend in some treatments indicates a possible mutually reducing interaction between chitosan and phenolic compounds at higher extract ratios. Although the extract contains active phenolic compounds, the compaction of the coating structure or changes in pH may limit the availability of these compounds to capture free radicals, thereby reducing antioxidant effectiveness. A pure chitosan solution has low antioxidant activity because there are no hydrogen atoms and free amino groups at the C-2 position [37]. The addition of extract gradually decreased the IC_{50} value, with the highest activity recorded in the 1.33% chitosan and 33.3% extract treatment, which was 4.43 ± 2.69 ppm. Other formulations with extract ratios of 20% and 33.3% showed IC_{50} values between 5.12 ± 0.33 and 6.31 ± 3.60 ppm, which are still relatively high. The decrease in IC_{50} indicates that phenolic compounds in the extract play an active role in neutralizing free radicals. However, their effectiveness depends on the balance between chitosan concentration and extract amount. An excessively high extract ratio has the potential to form phenolic-polymer complexes that reduce the availability of free active compounds, thereby inhibiting antioxidant activity. Formulations with a balanced composition are able to maintain matrix stability while increasing the antioxidant capacity of the system. In addition, DPPH

radical scavenging activity increased significantly with increasing concentrations of cinnamon essential oil [38]. The increase in phenolic compounds in essential oils also contributes to higher antioxidant capacity [39]. The addition of extracts or essential oils has a positive relationship with the total content of biologically degradable phenolics, thereby increasing antioxidant effectiveness and strengthening the ability to scavenge free radicals [40].

The ANOVA results (**Table 2**) show that the linear model is significant (p = 0.0253) in explaining the relationship between chitosan concentration and extract on the antioxidant activity of edible coatings. The chitosan concentration factor had no significant effect (p = 0.5217). In contrast, the extract factor was significant (p = 0.0091), confirming the dominance of phenolic compounds and flavonoids in the extract as antioxidants, while chitosan acted as a protective matrix. The insignificant *lack of fit* value (p = 0.6981) and *adequate precision* (0.5001) indicate model suitability and demonstrate the model's sensitivity to data variation. However, the R^2 (0.3876), *adjusted* R^2 (0.3059), and *predicted* R^2 (0.0650) indicate limitations in prediction, but the model's ability to explain response variation is adequate. The ANOVA results confirm that variations do not influence the variability of the antioxidant response in the composition of the chitosan extract, but the response mainly depends on bioactive compounds that remain relatively unchanged during liquid formulation. The 3D plot (**Figure 1(B)**) shows that antioxidant activity increases with increasing extract concentration, while the effect of chitosan is relatively small. The smooth surface and stable color gradation confirm the dominant role of the extract through the contribution of bioactive compounds, while chitosan only functions as a carrier matrix. The flat surface pattern with a slight increase indicates a stable linear relationship between the factors and the response, with the highest antioxidant activity in the combination of larger extracts. Equation 8 presents the regression equation that predicts antioxidant activity.

$$\text{Antioxidant activity} = 11.7169 - 0.5848A - 0.1816B \quad (8)$$

Antimicrobial activity

Variations in chitosan and extract concentrations affect the antimicrobial activity of edible coatings, mainly through the contribution of bioactive compounds such as phenolics and flavonoids. The inhibition mechanism involves cell membrane disruption, enzyme inhibition, and protein synthesis inhibition. Factors such as pH, viscosity, and solution homogeneity also determine the effectiveness of the system. Chitosan is known to have broad antimicrobial activity against pathogenic bacteria, including both Gram-positive and Gram-negative strains. The addition of natural extracts (garlic, red ginger, and red galangal) provides additional contributions through specific bioactive compounds contained in each extract. Antimicrobial tests were conducted on model bacteria *E. coli*, *S. aureus*, and *Salmonella* to assess the spectrum and intensity of activity. The results were then compared with those of controls without extract to evaluate the increase in effectiveness and identify differences in response between Gram-negative and Gram-positive bacteria.

Table 1 shows that the inhibition zone against *E. coli* (**Figure 2(A)**) increased significantly in the 2.67% chitosan formulation with the addition of 33.3% extract, compared to the control without extract ($p < 0.05$). The combination of medium chitosan with high-concentration extract produced a larger inhibition zone compared to the treatment without extract, indicating a combined effect between the 2 components. Increasing the amount of extract contributed more significantly to the effectiveness of E. coli inhibition than increasing the chitosan concentration alone. The optimal formulation must consider the balance between chitosan and extract to achieve the maximum E. coli inhibition zone while maintaining system stability. These results suggest that the bioactive components in the extract play a significant role in enhancing antimicrobial activity. At the same time, chitosan serves as a carrier matrix that facilitates the diffusion of active compounds. However, increasing chitosan and extract does not always increase effectiveness, possibly due to limited interaction of free amino groups with cell membranes or the formation of phenolic-polymer complexes that inhibit the release of free active compounds. The thin cell wall of *E. coli* facilitates the penetration of phenolic compounds, leading to membrane damage and leakage of cellular contents. At the same time, the positive charge of chitosan interacts with the negative charge of the bacterial membrane, accelerating cell structure damage.

Activity against the inhibition zone of *S. aureus* (**Figure 2(B)**) showed an increasing trend with the addition of 20% - 33.3% extract, although the variation between treatments was relatively small. Statistically, there were no significant differences between treatments ($p > 0.05$), so the trend of increasing inhibition zones against *S. aureus* was not strong enough to indicate a distinct treatment effect (**Table 1**). Compared to *E. coli*, the pattern of increase in the inhibition zone in *S. aureus* was more moderate, indicating that chitosan acts as a stable carrier matrix for bioactive compounds. At the same time, the extract contains phenolic components that can penetrate the membranes of Gram-positive bacteria. These results indicate that the addition of extract does not always increase inhibition activity when the diffusion of active compounds through the coating matrix is limited, or the density of the coating structure increases at higher chitosan concentrations. The structural properties of the *S. aureus* cell membrane play a greater role in determining effectiveness than the quantity of active components in the coating. This difference indicates that the thicker peptidoglycan wall structure of *S. aureus* tends to be more resistant to the penetration of active compounds than the lipopolysaccharide layer of *Salmonella*. The thick peptidoglycan structure in *S. aureus* acts as a physical barrier, reducing the penetration of phenolic compounds, making the primary mechanism more dependent on the ability of chitosan to adhere to the cell surface and increase membrane permeability. These findings confirm that the antimicrobial effectiveness against Gram-positive bacteria depends on the balance between the composition of chitosan and the extract, as well as the system's ability to maintain optimal diffusion of bioactive compounds.

A combination of 1.6% chitosan and 20% extract produced the largest inhibition zone against *Salmonella* (**Figure 2C**) and showed a significant difference from the extract-free control ($p < 0.05$). Increasing the extract concentration did not always result in additional activity, indicating that coatings with high chitosan concentrations tend to be too dense, thereby limiting the release of active compounds. This finding confirms that antimicrobial effectiveness against *Salmonella* depends on the balance between chitosan concentration and the extract's ability to diffuse through the coating matrix. The pattern of inhibition against *Salmonella* differed from that of the other 2 bacteria, with the highest effectiveness observed in the combination of low chitosan and moderate extract (**Table 1**), indicating that a specific composition allows for more optimal release of antimicrobial compounds. *Salmonella's* susceptibility to phenolic compounds is related to the extract's ability to damage the outer lipopolysaccharide membrane, a property similar to that of *E. coli*. However, *Salmonella's* sensitivity is more influenced by the coating viscosity, as the release of active compounds depends on the diffusion process. Increased activity against *Salmonella* correlates with the presence of bioactive compounds in the extract that are able to damage the membrane structure of Gram-negative bacteria more effectively. The balance between chitosan and extract concentrations is a key factor in designing an effective coating system to inhibit *Salmonella* growth.

The findings of antimicrobial activity against *E. coli*, *S. aureus*, and *Salmonella* in this study align with the report by Asghar *et al*. [41], which shows that antimicrobial activity against *E. coli*, *S. aureus*, and *Salmonella* increases with increasing concentrations of essential oils in film-forming solutions. The antimicrobial activity of edible coatings is evident from their ability to inhibit the growth of *E. coli*, *S. aureus*, and *Salmonella*, which demonstrates the effectiveness of the interaction between chitosan and bioactive compounds in edible coatings. Active compounds that play a role include allicin, ajoene, and aliphatic sulfides in garlic extract [42], antibacterial terpenoids such as zingerone, shogaol, nerolidol, and phenolic compounds in ginger extract [32], as well as flavonoids, saponins, phenols, and terpenes in galangal extract [43]. Incorporating ginger essential oil into composite films enhanced protection, stability, and bioactive compound preservation [44]. However, in this study, the antimicrobial activity of the combination of chitosan with a combination of garlic, red ginger, and red galangal extracts against Gram-positive bacteria (*S. aureus*) was slightly lower than that against Gram-negative bacteria, particularly *Salmonella*. These findings confirm that antimicrobial effectiveness depends not only on the amount of active compounds but also on the balance of composition and stability of the matrix. An optimal formulation can maintain a homogeneous distribution of bioactive compounds,

increase penetration of microbial targets, and maintain the stability of antimicrobial function in the matrix.

ANOVA analysis (**Table 2**) shows that the quadratic model is significant for *E. coli* ($p = 0.0114$; $R^2 = 0.6706$; *adjusted* $R^2 = 0.5334$; predicted $R^2 = 0.3152$; *adequate precision* = 7.4209; *lack of fit* = 0.9031). The response to *E. coli* was complex because the single effects of chitosan, extract, and their interaction were not significant ($p > 0.05$). These results confirm that a non-linear combination of components shapes antimicrobial activity against *E. coli*, rather than the direct influence of individual factors. The effectiveness of the model is moderate, reflecting that formulation prediction requires a complex approach that considers the synergy and concentration thresholds of active ingredients. Model 2FI is significant for *S. aureus* ($p = 0.0142$), with chitosan having a significant effect ($p = 0.0112$), the extract being insignificant ($p = 0.9751$), and the interaction between chitosan and extract being significant ($p = 0.0280$). R^2 value = 0.5193; *adjusted* $R^2 = 0.4163$; *predicted* $R^2 = 0.1700$; *adequate precision* = 5.8147; *lack of fit* = 0.7878. These results confirm that the synergy between polymers and bioactive compounds drives antimicrobial activity against *S. aureus*, rather than the composition of individual factors. Model validation is quite good, supporting the use of formulation combinations to enhance antimicrobial effectiveness selectively. Meanwhile, the quadratic model for *Salmonella* showed the highest significance ($p = 0.0012$), with $R^2 = 0.7807$; *adjusted* $R^2 = 0.6893$; *predicted* R^2 0.5350; *adequate precision* = 6.7020; *lack of fit* = 0.0239. These results confirm that the dynamics of the matrix structure and the distribution of active compounds shape the response to *Salmonella*, with non-linear effects playing a key role in optimizing inhibitory power. Despite a significant lack of fit, the model's predictive value and precision still support its use in formulation exploration. Scientifically, this pattern shows that *Salmonella* control requires a balance between active ingredient concentration and coating structure stability. Overall, the model is valid for all 3 bacteria. However, the prediction levels differ, with chitosan dominating in *S. aureus* and *Salmonella*, and the extract playing a greater role in *E. coli*. The plot 3D (**Figures 1(C) - 1(E)**) shows the interaction patterns of chitosan and extract concentrations on the inhibition zones of the 3 bacteria. In *E. coli*, an increase in both factors produces a non-linear pattern with a synergistic effect, supported by the ionic attraction between positively charged chitosan and phenolic compounds in the extract that damage the cell membrane. In *S. aureus*, the inhibition zone increases mainly through the role of chitosan and its synergy with the extract, in accordance with the characteristics of Gram-positive bacteria, which are more sensitive to ionic attachment mechanisms on the cell surface. In *Salmonella*, increasing chitosan concentration consistently enlarged the inhibition zone, while the extract acted as a supporter through phenolic activity that triggered excessive free radical formation within bacterial cells. This condition caused membrane damage and enzyme function disruption, thereby strengthening the inhibitory effect. The relatively smooth surface of the graph confirms the stability of the model and the consistency of the interaction between variables. The regression equations for predicting the antimicrobial activity of edible coatings are shown in Eqs. (9) - (11).

$$E.\ coli = 291.6306 - 216.8819A - 5.9916B + 2.2057AB + 36.1273A^2 + 0.0334B^2 \quad (9)$$

$$S.\ aureus = 2.7965 - 0.0385A + 0.1262B - 0.0476AB \quad (10)$$

$$Salmonella = -562.7594 + 423.5268A + 11.7616B - 4.3069AB - 70.5938A^2 - 0.0636B^2 \quad (11)$$

Characterization of edible coatings using Fourier transform infrared spectroscopy (FTIR)

FTIR spectroscopy characterizes the edible coatings by identifying the main functional groups involved in molecular interactions. **Figure 3** shows the FTIR spectrum that displays the characteristic absorption patterns of the coating layer from each treatment, followed by interpretation and identification of the FTIR absorption bands based on a comparison of the measured wave numbers with the characteristic range of functional groups listed in the standard organic spectroscopy literature [45]. The 2% chitosan treatment without extract had leading absorption bands at 3,327.89 - 3,330.76 cm^{-1} (-OH/N-H), 2,819.64 cm^{-1} (C-H in aliphatic compounds), 2,113.99 - 2,118.26 cm^{-1} (C≡C/C≡N), and 1,634.07 - 1,771.61 cm^{-1} (C=O/C=C). The addition of extracts at chitosan concentrations of 1.6% (20%) and 1.33% (33.3%) resulted in a shift of the

-OH and -NH bands to 3,327.82 - 3,350.46 cm^{-1}, indicating an increase in hydrogen bonding between chitosan and bioactive compounds. The phenolic band was more pronounced at 1,506.75 - 1,519.35 cm^{-1}, while the intensity of the C–O band (1,017.71 - 1,273.75 cm^{-1}) increased, indicating interaction between the polysaccharide and the active groups of the extract. In the 4% chitosan treatment without extract, the spectrum maintained the main band at 3,333.81 - 3,335.47 cm^{-1} (-OH/N-H), 2,114.95 - 2,120.37 cm^{-1} (C≡C/C≡N), and 1,634.54 - 1,637.12 cm^{-1} (C=O/C=C). The addition of extract at chitosan concentrations of 3.2% (20%) and 2.67% (33.3%) resulted in a shift of the -OH and -NH bands to 3,334.21 - 3,354.63 cm^{-1}, indicating stronger interactions compared to the 2% chitosan treatment. The phenolic band at 1,506.75 - 1,558.19 cm^{-1} appeared more intense, indicating the contribution of bioactive compounds from the extract to the stability of the edible coating structure. In addition, the absorption band at 1,271.42 - 1,153.88 cm^{-1} associated with C-O-C in polysaccharides underwent a slight shift, indicating a change in molecular interaction with the extract. The differences in spectrum between treatments show that increasing the concentration of chitosan and extract produces stronger intermolecular interactions, particularly through hydrogen bonds. These interactions strengthen the matrix structure and contribute to the physicochemical properties and barrier properties of the coating as a film. These results indicate that increasing the concentration of chitosan and extract not only adds active groups but also strengthens the matrix structure through chemical synergy between components.

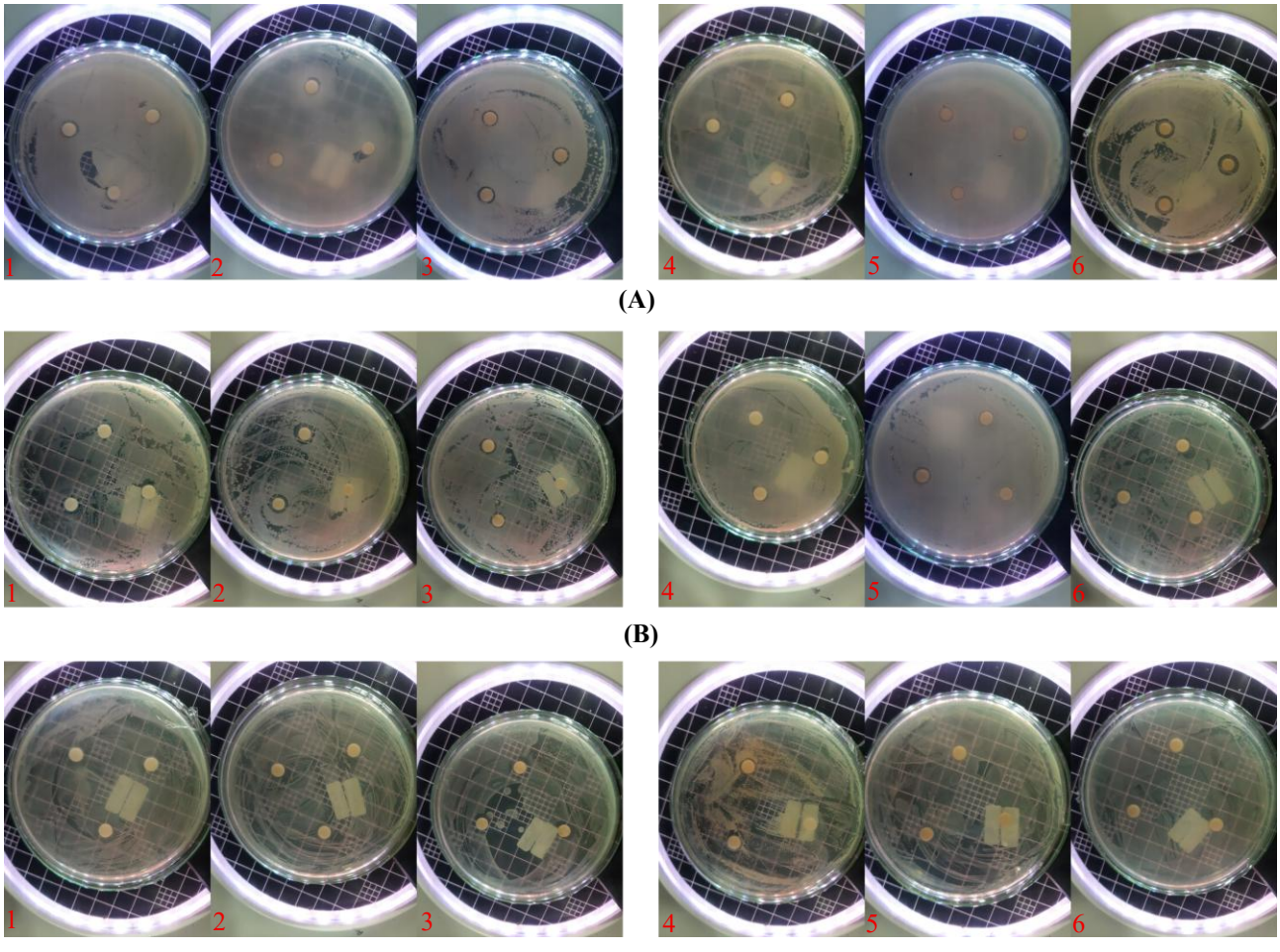

Figure 2 Antimicrobial activity of edible coatings based on inhibition zones against: (A) *E. coli*, (B) *S. aureus*, (C) *Salmonella*, (1) 2% chitosan with 0% extract, (2) 1.6% chitosan with 20% extract, (3) 1.33% chitosan with 33.3% extract, (4) 4% chitosan with 0% extract, (5) 3.2% chitosan with 20% extract, and (6) 2.67% chitosan with 33.3% extract.

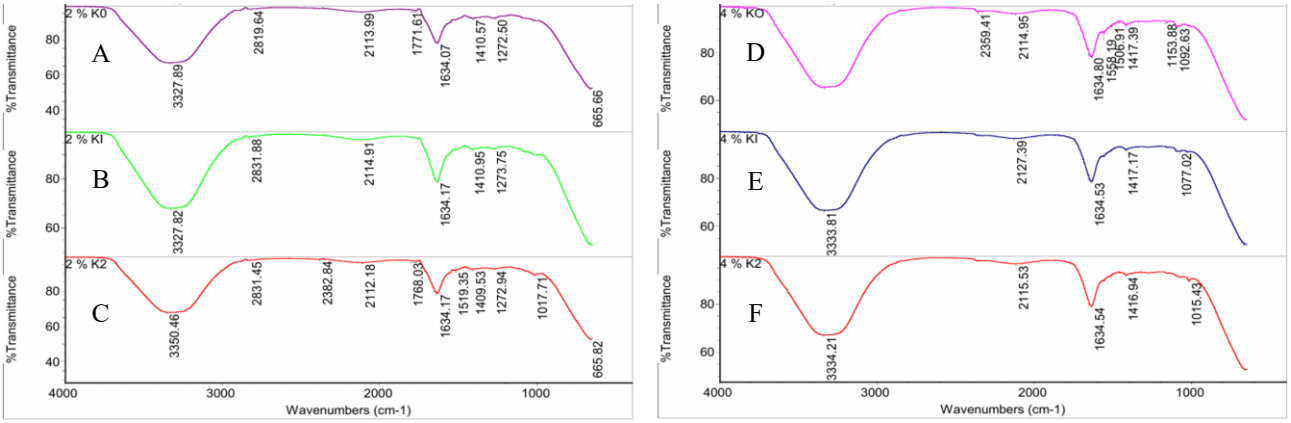

Figure 3 FTIR spectrum results of functional group identification in edible coatings: (A) 2% chitosan with 0% extract, (B) 1.6% chitosan with 20% extract, (C) 1.33% chitosan with 33.3% extract, (D) 4% chitosan with 0% extract, (E) 3.2% chitosan with 20% extract, and (F) 2.67% chitosan with 33.3% extract.

The results of the FTIR measurements obtained are in line with the findings of several studies that confirm the existence of chemical interactions and structural modifications in the chitosan-based edible coating matrix with the addition of extract, as indicated by the shift in the -OH strain at 3,286 - 3,404 cm^{-1} and the antisymmetric and symmetric COO- vibrations shifting from 1,585/1,425 to 1,590 - 1,594/1,409 - 1,412 cm^{-1} [15], followed by the O-H/N-H band at 3,000 - 3,500 cm^{-1}, carboxyl absorption at 2,923 cm^{-1}, aromatic/amino C=C band at 1,602 - 1,581 cm^{-1}, stretching from C-O 1,037 to 1,055 - 1,056 cm^{-1} with intensity 993 - 1,153 cm^{-1}, and phenolic groups at 1,624, 1,265, and 621 cm^{-1} [14]. The spectrum shows O-H/N-H stretching at 3,419 and 2,859 cm^{-1}, a shift in the amino N-H band from 1,657 - 1,598 cm^{-1} to 1,638 - 1,545 cm^{-1}, and C-O stretching at 993 - 1,153 cm^{-1} with a shift from 1,037 to 1,055 - 1,056 cm^{-1}, confirming hydrogen bonding and interactions between functional groups within the matrix [46], while the C≡N group absorption band appears at 2,100 - 2,250 cm^{-1} [47], including the ~2,115 cm^{-1} which is defined as carbodiimide strain and represents the vibration of triple-bonded groups (C≡C/C≡N) that are sensitive to the bond environment [48]. The broad O-H band (> 3,000 cm^{-1}), C-O absorption at 1,021 and 1,125 cm^{-1}, and C-H/ C=C band at 1,000 - 1,700 cm^{-1} overall indicate the consistency of functional groups in the chitosan film [12], thus strengthening the evidence of chemical interactions and structural modifications consistent with previous research reports.

The physical and functional characteristics of the edible film rely on thickness, tensile strength, elongation, and water vapor transmission rate (WVTR). **Table 3** presents the quantitative data for each treatment and offers a clear overview of the film's mechanical performance and moisture-barrier capability. **Figure 4** shows a response surface plot (3D) that illustrates the effect of chitosan, extract, and glycerol concentrations on the thickness, tensile strength, elongation, and WVTR of edible films. This visualization confirms the interaction between formulation variables that affect the physical and functional characteristics of the film. Furthermore, **Table 4** presents the results of ANOVA and RSM model regression used to predict and explain the relationship between formulation variables and the 4 parameters.

Table 3 Thickness, tensile strength, elongation, and WVTR of edible film.

Treatment			Parameter			
Chitosan concentration (% w/v)	**Extract (% v/v)**	**Glycerol addition**	**Thickness (mm)**	**Tensile strength (MPa)**	**Elongation (%)**	**WVTR (g day^{-1}m^{-2})**
2	0	Without glycerol	0.11 ± 0.00^{ab}	26.61 ± 14.64^{c}	9.63 ± 4.04^{bc}	350.52 ± 32.01^{ab}
1.6	20		0.11 ± 0.01^{ab}	5.92 ± 2.91^{a}	0.77 ± 0.40^{a}	326.83 ± 87.84^{ab}
1.33	33.3		0.22 ± 0.02^{d}	5.11 ± 0.76^{a}	1.87 ± 0.98^{ab}	318.95 ± 78.78^{ab}
2	0	With glycerol	0.11 ± 0.00^{ab}	10.08 ± 0.28^{ab}	14.37 ± 1.15^{c}	394.25 ± 35.30^{b}
1.6	20		0.09 ± 0.01^{a}	5.75 ± 1.37^{a}	8.80 ± 3.00^{abc}	292.90 ± 31.80^{ab}
1.33	33.3		0.18 ± 0.01^{cd}	5.01 ± 0.91^{a}	6.00 ± 0.89^{abc}	252.74 ± 40.30^{a}
4	0	Without glycerol	0.18 ± 0.00^{cd}	41.40 ± 4.12^{d}	9.67 ± 4.67^{bc}	326.76 ± 50.96^{ab}
3.2	20		0.22 ± 0.03^{d}	5.54 ± 2.36^{a}	1.57 ± 0.51^{ab}	300.30 ± 35.91^{ab}
2.67	33.3		0.34 ± 0.04^{e}	2.85 ± 0.56^{a}	0.67 ± 0.35^{a}	543.52 ± 49.36^{c}
4	0	With glycerol	0.17 ± 0.02^{cd}	20.28 ± 2.68^{bc}	32.77 ± 6.89^{d}	302.70 ± 40.17^{ab}
3.2	20		0.14 ± 0.01^{bc}	5.12 ± 1.56^{a}	4.67 ± 1.15^{ab}	410.32 ± 21.51^{bc}
2.67	33.3		0.19 ± 0.01^{d}	7.37 ± 0.53^{ab}	7.67 ± 0.35^{abc}	290.31 ± 14.67^{ab}

The data present values as mean ± SD (n = 3), and different lowercase letters in each column indicate significant differences ($p < 0.05$) according to Tukey's post-hoc test.

Thickness

Film thickness is one of the parameters used to assess the physical characteristics of edible films. Chitosan concentration, extract ratio, and glycerol content determine the thickness of the film. **Table 5** shows that film thickness differs significantly between treatments ($p < 0.05$), with film thickness increasing as the concentration of chitosan and extract increases. This increase indicates that the addition of solids from chitosan and active compounds in the extract strengthens the density of the polymer matrix, resulting in a thicker film structure. Films without extract showed the lowest thickness, indicating a more compact single-polymer structure. The addition of glycerol tended to increase thickness. However, it decreased the thickness in some formulations, reflecting the formation of a looser polymer network due to an increased distance between chains, resulting from a flexing effect and a decrease in structural density. These findings confirm that the interaction of the positive charge of the chitosan amine group with the phenolic compounds in the extract plays a crucial role in determining the thickness. At the same time, glycerol tends to weaken the hydrogen bonds within the matrix. This interaction aligns with the opinion of Ren *et al*. [49], stating that phenolic compounds in the extract form hydrogen and ionic bonds with the chitosan's amine group, thereby increasing the film dimensions. The addition of spice extracts and plasticizers also affects the moisture content in the matrix and the hydrophilic properties of the film through the formation of covalent bonds between polyphenols and water molecules [12]. The thickness of the resulting film meets the Japan Industrial Standard (JIS), with a maximum limit of 0.25 mm [32].

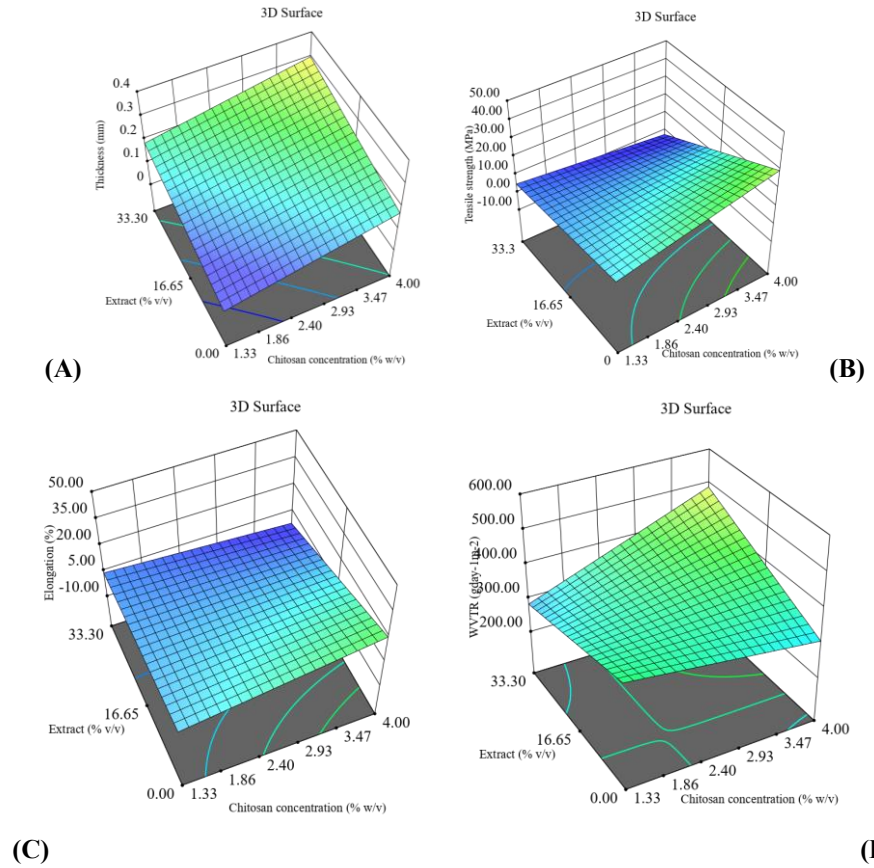

Figure 4 Surface response plot of the effect of chitosan, extract, and glycerol concentrations on: (A) thickness, (B) tensile strength, (C) elongation, and (D) WVTR.

Tensile strength and elongation

The tensile strength test measures the maximum force required to stretch the film to the point of breakage, while the elongation test assesses the film's ability to undergo elongation. **Table 5** shows that the tensile strength values differ significantly between treatments ($p < 0.05$), with the tensile strength of the film decreasing significantly in formulations with higher extract concentrations and in treatments with glycerol. This mechanism can be explained by the phenolic compounds in the extract disrupting the regularity of the chitosan chains, thereby reducing the stiffness of the polymer network. The addition of glycerol enhances this effect by increasing chain mobility and reducing the degree of crystal regularity. Conversely, films with high chitosan concentrations without glycerol exhibit the highest tensile strength, reflecting the dominance of hydrogen bonds and stronger interactions between polysaccharides. Increasing the chitosan concentration and adding glycerol strengthened the bonds between polymer chains, thereby increasing tensile strength [50]. At the same time, the extract tended to weaken the structure and reduce the mechanical strength of the film [15].

The elongation values in **Table 5** show that the differences between treatments are significant ($p < 0.05$), with elongation increasing significantly in films containing glycerol and extract. This increase is likely due to the formation of a more flexible structure resulting from weakened intermolecular bonds and increased space between polymer chains. Conversely, films without glycerol tended to be brittle with low elongation values, especially in formulations with high tensile strength. Glycerol increases the elongation of chitosan films, acting as a plasticizer that enhances film flexibility by promoting greater mobility of the polymer chains. The use of glycerol was also followed by a decrease in tensile strength, indicating a reduction in film structure stiffness. These results are in line with the opinion of Haddar *et al*. [51], which states that the

addition of glycerol can soften the chitosan structure by weakening hydrogen bonds and increasing film flexibility. The treatment of 2.67% chitosan and 33.3% extract without glycerol produced the lowest elongation because the high ratio of extract without glycerol weakened the interchain bonds and reduced elasticity [50]. The addition of extract increases the stiffness of the film, while glycerol plays a role in increasing elasticity [52]. Formulation and film thickness directly influence tensile strength, whereas elongation decreases as tensile strength increases. Films with high tensile strength are able to withstand pressure, while high elongation values reflect good elasticity [53]. Most treatments produced tensile strength that met JIS standards, while only a few treatments showed elongation values above the threshold of acceptability [32]. These findings show that the formulation strongly controls flexibility, even when the film achieves optimal tensile strength. The inverse relationship between tensile strength and elongation shows that the film gains flexibility when its structural resistance decreases.

Table 4 ANOVA results and RSM model regression for thickness, tensile strength, elongation, and WVTR prediction.

Response	Thickness	Tensile strength	Elongation	WVTR
Model (Reduction/Transformation)	2FI	2FI	2FI	2FI
Model (*p*-value)	< 0.0001	< 0.0001	< 0.0001	0.0112
Chitosan concentration (A)	< 0.0001	0.0964	0.1864	0.0837
Extract (B)	< 0.0001	< 0.0001	< 0.0001	0.1804
Glycerol addition (C)	0.0004	0.0018	< 0.0001	0.1572
AB	0.8334	0.0008	0.0015	0.0047
AC	0.0431	0.8545	0.0320	0.5177
BC	0.0011	0.0002	0.2240	0.0127
Lack of fit (*p*-value)	< 0.0001	0.0205	0.0001	0.0001
R^2	0.7623	0.8274	0.8030	0.4146
Adjusted R^2	0.7132	0.7917	0.7623	0.2934
Predicted R^2	0.6529	0.7173	0.6819	0.1438
Adequate precision	13.8320	16.4146	16.3076	6.7328

na = not applicable, R^2 = coefficient of determination

Water vapor transmission rate (WVTR)

Barrier characteristic testing is required to assess the permeability of edible films to O_2, CO_2, water vapour, and liquids. **Table 5** shows that the WVTR values differ significantly between treatments ($p < 0.05$), with WVTR decreasing in films with high chitosan concentration without glycerol. Such conditions indicate that a denser and more homogeneous polymer matrix forms, along with strong hydrogen bonds, thereby limiting the pathways for water vapour diffusion. The addition of extract to low chitosan can also significantly reduce WVTR, indicating structural reinforcement through polyphenol-chitosan interactions. Low-chitosan film formulations with the addition of extract and glycerol have improved oxygen barrier properties through reduced water vapor permeability. However, at higher extract concentrations, especially with the addition of glycerol, the WVTR increases again because the regularity of the matrix is disrupted, thereby increasing permeability. Glycerol can consistently increase the WVTR in all treatments, indicating an expansion of the distance between polymer chains and increased molecular mobility, thereby opening up the water vapor diffusion pathway.

The hygroscopic nature of glycerol makes the film more susceptible to water absorption, thereby reducing its effectiveness in inhibiting water vapor transmission. These results confirm that the balance between chitosan, extract concentration, and glycerol composition governs WVTR effectiveness, as chitosan strengthens the structure, extracts can either reinforce or weaken the matrix depending on their level, and glycerol increases flexibility but reduces resistance to water vapor transmission. The addition of extract and glycerol in the right concentrations formed a solid film matrix that produced hydrophobic points and reduced hydrophilic groups, thereby decreasing water vapor permeability [46]. Conversely, glycerol at high concentrations increases hydrophilic properties and opens spaces between polymers, thereby increasing WVTR [14]. Chitosan formulations with extracts tend to decrease WVTR due to the dominance of hydrophobic components that inhibit water vapor transfer [54]. The interaction between the chitosan network and phenolic compounds from essential oils also reduces the availability of hydrophilic groups in the film matrix [55]. Films with low permeability are recommended as packaging materials because they effectively inhibit oxygen diffusion [56].

Analysis of edible film properties using RSM

ANOVA analysis (**Table 4**) shows that the 2-factor interaction model (2FI) is significant for all 4 edible film properties. For thickness, the model is valid ($p < 0.0001$), with the factors of chitosan concentration, extract, and glycerol having a significant effect ($p < 0.0001$; $p < 0.0001$; $p = 0.0004$). The AC (0.0431) and BC (0.0011) interactions were significant, while AB had no significant effect ($p = 0.8334$). The values $R^2 = 0.7623$; *adjusted* $R^2 = 0.7132$; *predicted* $R^2 = 0.6529$; *adequate precision* = 13.8320 confirmed the suitability of the model, despite a significant *lack of fit* ($p < 0.0001$). The ANOVA model indicates that the 2FI model is a significant predictor of film thickness variation. Chitosan and extract factors play a dominant role with linear effects, while glycerol contributes less but is still significant. The chitosan-glycerol and extract-glycerol interactions are proven to affect thickness through changes in the distance between polymer chains. For tensile strength, the model is significant ($p < 0.0001$) with extract as the dominant factor ($p < 0.0001$), glycerol has a significant effect ($p = 0.0018$), while chitosan is not significant ($p = 0.0964$). The AB ($p = 0.0008$) and BC ($p = 0.0002$) interactions were significant, while AC had no significant effect ($p = 0.8545$). The values $R^2 = 0.8274$; *adjusted* $R^2 = 0.7917$; *adequate precision* = 16.4146 4146 indicate high accuracy, with a significant *lack of fit* ($p = 0.0205$). The ANOVA model indicates that the 2FI model is significant, with extract and glycerol having a significant effect on tensile strength. In contrast, chitosan, considered as a single factor, has no significant effect. The interaction between factors proves that the effect of composition is not simply additive but depends on the combination of polymer structure with extract and glycerol. The high validity of the regression model confirms the consistency of the relationship between variables and the predictive ability of the formulation.

For elongation, the model was significant ($p < 0.0001$), with extract and glycerol having a significant effect ($p < 0.0001$), while chitosan was not significant ($p = 0.1864$). The interactions AB ($p = 0.0015$) and AC ($p = 0.0320$) are significant, while BC is not significant ($p = 0.2240$). The values $R^2 = 0.8030$; *adjusted* $R^2 = 0.7623$; *predicted* $R^2 = 0.6819$, *adequate precision* = 16.3076, confirm the suitability and stability of the model, despite a significant *lack of fit* ($p = 0.0001$). The ANOVA model indicates that extract and glycerol have a significant effect on elongation, while chitosan does not contribute significantly as a single factor. The interactions between chitosan extract and extract-glycerol are proven to be important, indicating that changes in the internal structure of the film depend on the combination of biopolymers and the effective degree of flexibility. The high validity of the regression model confirms the consistency of the relationship between variables and the predictive ability of the formulation. For WVTR, the model is significant ($p = 0.0112$), although the single factors chitosan, extract, and glycerol are not significant ($p = 0.0837$; $p = 0.1804$; $p = 0.1572$). The interactions AB ($p = 0.0047$) and BC ($p = 0.0127$) are significant, while AC is not significant ($p = 0.5177$). The values $R^2 = 0.4146$; *adjusted* $R^2 = 0.2934$; *predicted* $R^2 = 0.1438$; *adequate precision* = 6.7328 indicate moderate predictive ability, with a significant *lack of fit* ($p = 0.0001$). The 2FI ANOVA model indicates that WVTR is less sensitive to single factors; however, the interactions between chitosan-extract and

chitosan-glycerol have a significant effect. The evidence confirms that barrier capability depends more on the structural integration between components than on individual composition. Visualization of response surface plots (**Figures 4(A) - 4(D)**) confirms the interaction between formulation variables. Increasing chitosan thickens the film and decreases WVTR. The extract acts as a natural plasticizer that increases elongation but decreases tensile strength, while glycerol enhances flexibility but increases WVTR. The smooth graph surface and stable color gradation indicate a consistent response pattern, with the optimal combination of high chitosan, moderate extract, and controlled glycerol producing the best balance between thickness, tensile strength, elongation, and WVTR. The regression equations for predicting thickness, tensile strength, elongation, and WVTR appear in Eqs. (12) - (15).

$$\text{Thickness} = -0.0500 + 0.0597A + 0.0058B + 0.0924C - 0.0001AB - 0.0308AC - 0.0036BC \quad (12)$$

$$\text{Tensile strength} = 11.1902 + 6.9094A - 0.1529B - 16.0573C - 0.2865AB - 0.4060AC + 0.6428BC \quad (13)$$

$$\text{Elongation} = 0.7946 + 2.7990A + 0.2515B + 1.3079C - 0.2131AB + 3.9107AC - 0.1466BC \quad (14)$$

$$\text{WVTR} = 356.7650 - 15.2427A - 4.1877B + 99.8822C + 3.0466AB - 18.6249AC - 5.1342BC \quad (15)$$

Conclusions

This study confirms that the formulation interaction between chitosan and botanical extracts is a key factor determining the functional performance of edible coatings and edible films, through a synergistic mechanism that strengthens the polymer matrix structure and enhances bioactivity. These findings offer new insights into the contribution of chitosan-extract composition to the structural stability and functional efficiency of coatings, as demonstrated by their physical, chemical, and bioactive characteristics, as well as FTIR analysis. The best formulation, namely 1.33% chitosan combined with 33.3% extract, resulted in a pH of 4.31, IC50 4.43 ppm, inhibition zones against *E. coli* 2.32 mm, *S. aureus* 4.70 mm, *Salmonella* 5.23 mm, thickness 0.18 mm, tensile strength 5.01 MPa, elongation 6.00%, and WVTR 252.74 $g \cdot day^{-1}m^{-2}$. The FTIR spectrum showed a shift in -OH/-NH (3,327 - 3,355 cm^{-1}), an increase in the phenolic band (1,506 - 1,558 cm^{-1}), and C-O intensity (1,017 - 1,274 cm^{-1}), indicating hydrogen interaction and the contribution of bioactive compounds in the extract to the stability of the coating. Additionally, modelling using RSM with a custom design approach produced a predictive equation that shows the role of interactions between formulation variables on coating material performance. These findings make significant scientific contributions to the development of biomaterial-based coating systems by providing a theoretical basis and predictive approach that enable the formulation of more efficient systems without relying on trial-and-error methods. Practically, this research recommends edible coatings and films based on chitosan and botanical extracts as alternatives for sustainable, environmentally friendly food packaging systems. To ensure wider application, further studies are needed for industrial-scale evaluation, application testing on real food commodities, and long-term storage stability before commercial implementation.

Acknowledgements

The author would like to thank the Indonesian Education Scholarship, the Center for Higher Education Funding and Assessment, Ministry of Higher Education, Science, and Technology of the Republic of Indonesia, and the Endowment Fund for Education Agency, Ministry of Finance of the Republic of Indonesia, for providing financial support that enabled this research to be completed successfully (Decree Number 00302/J5.2.3./BPI.06/9/2022, BPI ID: 202209090788).

Declaration of generative AI in scientific writing

The authors declare that artificial intelligence-based tools, such as Grammarly and ChatGPT by OpenAI, were used solely to support language editing and grammar correction during the manuscript writing process. These tools generated no content or data interpretation. The entire content and conclusions in this work are solely the responsibility of the authors.

CRediT author statement

Edo Saputra: Conceptualization; Methodology; Software; Validation; Formal analysis; Investigation;

Resources; Data Curation; Writing - Original Draft; Writing - Review & Editing; Visualization. **Rokhani Hasbullah**: Supervision; Validation; Data curation; Writing - Review & Editing; Visualization. **Emmy Darmawati**: Supervision; Writing - Review & Editing; Visualization. **Mala Nurilmala**: Supervision; Writing - Review & Editing; Visualization.

References

[1] A Matloob, H Ayub, M Mohsin, S Ambreen, FA Khan, S Oranab, MA Rahim, W Khalid, GA Nayik, S Ramniwas and S Ercisli. A review on edible coatings and films: advances, composition, production methods, and safety concerns. *American Chemical Society Omega* 2023; **8(32)**, 28932-28944.

[2] D Castro, A Podshivalov, A Ponomareva and A Zhilenkov. Study of the reinforcing effect and antibacterial activity of edible films based on a mixture of chitosan/cassava starch filled with bentonite particles with intercalated ginger essential oil. *Polymers* 2024; **16(17)**, 2531.

[3] P Cazón, E Morales-Sanchez, G Velazquez and M Vázquez. Measurement of the water vapor permeability of chitosan films: A laboratory experiment on food packaging materials. *Journal of Chemical Education* 2022; **99**, 2403-2408.

[4] A Jiang, R Patel, B Padhan, S Palimkar, P Galgali, A Adhikari, I Varga and M Patel. Chitosan based biodegradable composite for antibacterial food packaging application. *Polymers* 2023; **15(10)**, 2235.

[5] LA Picos-Corrales, AM Morales-Burgos, JP Ruelas-Leyva, G Crini, E García-Armenta, SA Jimenez-Lam, LE Ayón-Reyna, F Rocha-Alonzo, L Calderón-Zamora, U Osuna-Martínez, A Calderón-Castro, G De-Paz-Arroyo and LN Inzunza-Camacho. Chitosan as an outstanding polysaccharide improving health-commodities of humans and environmental protection. *Polymers* 2023; **15(3)**, 526.

[6] S Ma, Y Zheng, R Zhou and M Ma. Characterization of chitosan films incorporated with different substances of konjac glucomannan, cassava starch, maltodextrin and gelatin, and application in mongolian cheese packaging. *Coatings* 2021; **11(1)**, 84.

[7] BH Ulusoy, FK Yildirim and C Hecer. Edible films and coatings: A good idea from past to future technology. *Journal of Food Technology Research* 2018; **5(1)**, 28-33.

[8] M Barik, G BhagyaRaj, KK Dash and R Shams. A thorough evaluation of chitosan-based packaging film and coating for food product shelf-life extension. *Journal of Agriculture and Food Research* 2024; **16**, 101164.

[9] C Antonino, G Difonzo, M Faccia and F Caponio. Effect of edible coatings and films enriched with plant extracts and essential oils on the preservation of animal-derived foods. *Journal of Food Science* 2024; **89(2)**, 748-772.

[10] W Chang, F Liu, HR Sharif, Z Huang, HD Goff and F Zhong. Preparation of chitosan films by neutralization for improving their preservation effects on chilled meat. *Food Hydrocolloids* 2019; **90**, 50-61.

[11] NE Suyatma, S Gunawan, RY Putri, A Tara, F Abbès, DY Hastati and B Abbès. Active biohybrid nanocomposite films made from chitosan, ZnO nanoparticles, and stearic acid: Optimization study to develop antibacterial films for food packaging application. *Materials* 2023; **16(3)**, 926.

[12] K Venkatachalam, N Rakkapao and S Lekjing. Physicochemical and antimicrobial characterization of chitosan and native glutinous rice starch-based composite edible films: Influence of different essential oils incorporation. *Membranes* 2023; **13(2)**, 161.

[13] F Handayasari, NE Suyatma and S Nurjanah. Physiochemical and antibacterial analysis of gelatin-chitosan edible film with the addition of nitrite and garlic essential oil by response surface methodology. *Journal of Food Processing and Preservation* 2019; **43(12)**, e14265.

[14] A Al-Harrasi, S Bhtaia, MS Al-Azri, HA Makeen, M Albratty, HA Alhazmi, S Mohan, A Sharma and T Behl. Development and characterization of chitosan and porphyran based composite edible films containing ginger essential oil. *Polymers* 2022; **14(9)**, 1782.

[15] W Zhou, Y He, F Liu, L Liao, X Huang, R Li, Y Zou, L Zhou, L Zou, Y Liu, R Ruan and J Li. Carboxymethyl chitosan-pullulan edible films enriched with galangal essential oil:

Characterization and application in mango preservation. *Carbohydrate Polymers* 2021; **256**, 117579.

[16] A Irawan, DR Barleany, J Jayanudin, M Yulivianti, D Desiana and F Haqi. Antimicrobial activity of chitosan based edible film enriched with red ginger essential oil as an active packaging for food. *Research Journal of Pharmaceutical, Biological and Chemical Sciences* 2017; **8(3)**, 1523-1530.

[17] S Mishra, S Mullasseri, R Mishra, A Saha, MS Induja and D Madduru. Chitosan biopolymer film with garlic peel extract. *Current Science* 2022; **122**, 12-15.

[18] SA Al-Hilifi, RM Al-Ali and AT Petkoska. Ginger essential oil as an active addition to composite chitosan films: development and characterization. *Gels* 2022; **8(6)**, 327.

[19] Y Cao, W Gu, J Zhang, Y Chu, X Ye, Y Hu and J Chen. Effects of chitosan, aqueous extract of ginger, onion and garlic on quality and shelf life of stewed-pork during refrigerated storage. *Food Chemistry* 2013; **141**, 1655-1660.

[20] Y Levania, Michael and EA Prasetyanto. Chitosan and red ginger extract patches for diabetic foot ulcers: An alternative for urban healthcare challenges. *Jurnal Perkotaan* 2025; **17(1)**, 38-45.

[21] R Elsabagh, SS Ibrahim, EM Abd-Elaaty, A Abdeen, AM Rayan, SF Ibrahim, M Abdo, F Imbrea, L Şmuleac, AM El-Sayed, RY Abd Elghaffar and MK Morsy. Chitosan edible coating: a potential control of toxic biogenic amines and enhancing the quality and shelf life of chilled tuna filets. *Frontiers in Sustainable Food Systems* 2023; **7**, 1-12.

[22] NA Pratiwi, I Rostini, A Yustiati and RA Pratama. Effect of red ginger essential oil (*Zingiber officinale Var*. *Rubrum*) addition on chitosan based edible coating towards organoleptic characteristics pempek. *Asian Journal of Fisheries and Aquatic Research* 2021; **15(5)**, 1-9.

[23] SH Nofiyanti, LDR Fajarini, IGAM Putra and YLV Arista. Process intensification of polyphenol and flavonoid extraction from ant nest (*Myrmecodia pendans*) via ohmic heating: Investigating joule heating and electric field-time interactions using a response surface methodology. *Trends in Sciences* 2025; **22(11)**, 10471.

[24] JO Akullo, B Kiage, D Nakimbugwe and J Kinyuru. Effect of aqueous and organic solvent extraction on in-vitro antimicrobial activity of 2 varieties of fresh ginger (*Zingiber officinale*) and garlic (*Allium sativum*). *Heliyon* 2022; **8(9)**, e10457.

[25] MW Apriliyani, Purwadi, A Manab, BM Ahmad and LM Uula. Physico-chemical and antimicrobial properties of caseinchitosan edible films as food quality and food safety Physico-chemical and antimicrobial properties of casein- chitosan edible films as food quality and food safety. *IOP Conference Series: Earth and Environmental Science* 2020; **443**, 012018.

[26] JMF Pavoni, CL Luchese and IC Tessaro. Impact of acid type for chitosan dissolution on the characteristics and biodegradability of cornstarch/chitosan based films. *International Journal of Biological Macromolecules* 2019; **138**, 693-70.

[27] A Pavinatto, AV de A Mattos, ACG Malpass, MH Okura, DT Balogh and RC Sanfelice. Coating with chitosan-based edible films for mechanical/biological protection of strawberries. *International Journal of Biological Macromolecules* 2019; **151**, 1004-1011.

[28] A Pažarauskait˙e, EN Fernández, I Sone, M Sivertsvik and N Sharmin. Combined effect of citric acid and polyphenol-rich grape seed extract towards bioactive smart food packaging systems. *Polymers* 2023; **15(14)**, 3118.

[29] H Dysjaland, I Sone, EN Fernández, M Sivertsvik and N Sharmin. Mechanical, barrier, antioxidant and antimicrobial properties of alginate films: Effect of seaweed powder and plasma-activated water. *Molecules* 2022; **27(23)**, 8356.

[30] T Ganić, S Vuletić, B Nikolić, M Stevanović, M Kuzmanović, D Kekić, S Đurović, S Cvetković and D Mitić-Ćulafić. Cinnamon essential oil and its emulsion as efficient antibiofilm agents to combat *Acinetobacter baumannii*. *Frontiers in Microbiology* 2022; **13**, 989667.

[31] D Wang, J Sun, J Li, Z Sun, F Liu, L Du and D Wang. Preparation and characterization of gelatin/zein nanofiber films loaded with

perillaldehyde, thymol, or ε-polylysine and evaluation of their effects on the preservation of chilled chicken breast. *Food Chemistry* 2022; **373**, 131439.

[32] D Silvia, Zulkarnain, RI Fadhilah, H Kamilah and NNAK Shah. Effect of ginger (*Zingiber officinale*) extracts on mechanical and antimicrobial properties of ganyong starch edible films as primary packaging of crabstick. *Trends in Sciences* 2024; **21(7)**, 7711.

[33] X Guo, C Ren, Y Zhang, H Cui and C Shi. Stability of zein-based films and their mechanism of change during storage at different temperatures and relative humidity. *Journal of Food Processing and Preservation* 2020; **44(9)**, e14671.

[34] H Du, C Liu, O Unsalan, C Altunayar-Unsalan, S Xiong, A Manyande and H Chen. Development and characterization of fish myofibrillar protein/chitosan/rosemary extract composite edible films and the improvement of lipid oxidation stability during the grass carp fillets storage. *International Journal of Biological Macromolecules* 2021; **184**, 463-475.

[35] E Díaz-montes and R Castro-muñoz. Trends in chitosan as a primary biopolymer for functional films and coatings manufacture for food and natural products. *Polymers* 2021; **13(5)**, 767.

[36] S Khan, AAA Abdo, Y Shu, Z Zhang and T Liang. The extraction and impact of essential oils on bioactive films and food preservation, with emphasis on antioxidant and antibacterial activities-A review. *Foods* 2023; **12(22)**, 4169.

[37] M Flórez, E Guerra-Rodríguez, P Cazón and M Vázquez. Chitosan for food packaging: Recent advances in active and intelligent films. *Food Hydrocolloids* 2022; **124**, 107328.

[38] S Ghani, H Barzegar, M Noshad and M Hojjati. The preparation, characterization and in vitro application evaluation of soluble soybean polysaccharide films incorporated with cinnamon essential oil nanoemulsions. *International Journal of Biological Macromolecules* 2018; **112**, 197-202.

[39] A Tügen, B Ocak and Ö Özdestan-Ocak. Development of gelatin/chitosan film incorporated with lemon essential oil with antioxidant properties. *Journal of Food Measurement and Characterization* 2020; **14**, 3010-3019.

[40] RM Al-Ali, SA Al-Hilifi and MMA Rashed. Fabrication, characterization, and anti-free radical performance of edible packaging-chitosan film synthesized from shrimp shell incorporated with ginger essential oil. *Journal of Food Measurement and Characterization* 2021; **15**, 2951-2962.

[41] L Asghar, A Sahar, MI Khan and M Shahid. Fabrication and characterization of chitosan and gelatin-based antimicrobial films incorporated with different essential oils. *Foods* 2024; **13(12)**, 1796.

[42] SB Bhatwalkar, R Mondal, SBN Krishna, JK Adam, P Govender and R Anupam. Antibacterial properties of organosulfur compounds of garlic (*Allium sativum*). *Frontiers in Microbiology* 2021; **12**, 613077.

[43] IM Aziz, AA Alfuraydi, OM Almarfadi, MAM Aboul-Soud, AK Alshememry, AN Alsaleh and FN Almajhdi. Phytochemical analysis, antioxidant, anticancer, and antibacterial potential of *Alpinia galanga* (L.) rhizome. *Heliyon* 2024; **10(17)**, e37196.

[44] A Amalraj, JT Haponiuk, S Thomas and S Gopi. Preparation, characterization and antimicrobial activity of polyvinyl alcohol/gum arabic/chitosan composite films incorporated with black pepper essential oil and ginger essential oil. *International Journal of Biological Macromolecules* 2020; **151**, 366-375.

[45] T Hong, JY Yin, SP Nie and MY Xie. Applications of infrared spectroscopy in polysaccharide structural analysis: Progress, challenge and perspective. *Food Chemistry* 2021; **12**, 100168.

[46] VS dos Santos, MV Lorevice, GS Baccarin, FM da Costa, R da Silva Fernandes, FA Aouada and MR de Moura. Combining chitosan nanoparticles and garlic essential Oil as additive fillers to produce pectin-based nanocomposite edible films. *Polymers* 2023; **15(10)**, 2244.

[47] MG Maienschein-Cline and CH Londergan. The CN stretching band of aliphatic thiocyanate is sensitive to solvent dynamics and specific solvation. *The Journal Physical Chemistry A Letters* 2007; **111(40)**, 10020-10025.

[48] A Sarhan. Characterization of chitosan and

polyethylene glycol blend film. *Egyptian Journal of Chemistry* 2019; **62(12)**, 405-412.

[49] B Karkar, S Şahin, D Bekiz, B Akça and C Özakın. Evaluation of antioxidant films of chitosan with *Aquilaria agallocha* extract as packaging material. *Journal of Food Science* 2023; **88**, 2571-2582.

[50] YY Ren, JL Fang, RZ Gong, ZL Xiang and PP Sun. Preparation of alkali-soluble polysaccharide from *Clausena lansium* (Lour.) skeels and its effects on properties of chitosan-based edible film. *Frontiers in Sustainable Food Systems* 2023; **7**, 1185951.

[51] A Haddar, E Sellami, O Bouazizi, A Sila and A Bougatef. Biodegradable levan/chitosan composite films: Development and application in beef filet packaging. *Foods* 2025; **14(12)**, 2133.

[52] J Wang, M Ismail, NR Khan, DEN Khan, T Iftikhar, MG Shahid, SU Shah and ZU Rehman. Chitosan based ethanolic Allium sativum extract hydrogel film: A novel skin tissue regeneration platform for 2nd degree burn wound healing. *Biomedical Materials* 2024; **19(4)**, 045036.

[53] M Elma, EA Pradana, N Sihombing, RN Thala'ah, A Rahma and ELA Rampun. Edible film fabrication derived from nagara starch and ded ginger essential oil as a package of instant noodles seasoning. *IOP Conference Series: Earth and Environmental Science* 2022; **999**, 012024.

[54] A Zehra, SM Wani, N Jan, TA Bhat, SA Rather, AR Malik and SZ Hussain. Development of chitosan-based biodegradable films enriched with thyme essential oil and additives for potential applications in packaging of fresh collard greens. *Scientific Reports* 2022; **12(1)**, 16923.

[55] Z Shen and DP Kamdem. Development and characterization of biodegradable chitosan films containing 2 essential oils. *International Journal of Biological Macromolecules* 2015; **74**, 289-296.

[56] P Cazón and M Vázquez. Mechanical and barrier properties of chitosan combined with other components as food packaging film. *Environmental Chemistry Letters* 2019; **18(2)**, 257-267.